

Piezoelectric properties of zirconium-doped barium titanate single crystals grown by templated grain growth

Paul W. Rehrig,^{a)} Seung-Eek Park, Susan Trolier-McKinstry, Gary L. Messing, Beth Jones, and Thomas R. ShROUT

Materials Research Laboratory, The Pennsylvania State University, University Park, Pennsylvania 16802

(Received 25 January 1999; accepted for publication 21 April 1999)

Single crystals of $\text{Ba}(\text{Zr}_x\text{Ti}_{1-x})\text{O}_3$ were grown by templated grain growth (TGG). Millimeter size single crystals of $\text{Ba}(\text{Zr}_x\text{Ti}_{1-x})\text{O}_3$ were produced by heating a BaTiO_3 crystal in contact with a sintered polycrystalline matrix of 4.5, 5.0, or 8.5 mol % Zr-doped barium titanate for 30 h at 1350 °C. To facilitate boundary migration, the ceramic compact was made 3 mol % TiO_2 excess. The 4.5 and 5.0 mol % Zr-doped crystals were orthorhombic at room temperature, and for a pseudocubic (001) orientation, they showed remanent polarizations of 13 $\mu\text{C}/\text{cm}^2$ and a high field d_{33} of 340–355 pC/N. The 8.5 mol % Zr-doped crystal [again oriented along the pseudocubic (001)] was rhombohedral at room temperature with a remanent polarization of 10 $\mu\text{C}/\text{cm}^2$. A k_{33} value of 0.74 from resonance measurements was observed for the 4.5 mol % Zr-doped crystal. © 1999 American Institute of Physics. [S0021-8979(99)02815-7]

I. INTRODUCTION

Ultrahigh electrically induced strain levels (up to 1.7%) were recently discovered in lead-based relaxor ferroelectric single crystals.¹ The composition of these perovskite crystals lies near a morphotropic phase boundary (MPB) between tetragonal and rhombohedral phases. It was found that lead zinc niobate–lead titanate and lead magnesium niobate–lead titanate rhombohedral crystals oriented and poled along the pseudocubic [001] axis had an enhanced piezoelectric response compared to [111] oriented crystals (which is the polar axis direction), which was related to crystallographic engineering.^{1,2} These enormous strain levels, coupled with the large piezoelectric constants and electromechanical coupling coefficients are extremely attractive for a variety of sensor and actuator applications. Another important result of crystallographic engineering is a low level of hysteresis in the strain, at least to strain levels on the order of 0.6%. This is believed to be due to the fact that the four domain states in a poled crystal are equally favored by an applied electric field, so that there is no driving force for extensive domain wall motion. Hence, the question arises, “Is this concept of crystallographic engineering applicable to other ferroelectric crystals?”

Initial work on BaTiO_3 indicates that the concept of crystallographic engineering can be applied to this system as well.³ Piezoelectric coefficient, d_{33} , values up to 420 and 300 pC/N observed in orthorhombic (0 °C) and rhombohedral (–100 °C) crystals poled along the pseudocubic [001], appreciably higher than those measured for the tetragonal phase at room temperature (~125 pC/N), are the result of crystallographic engineering. This suggests that improved piezoelectric properties can be achieved in non-lead-based perovskite crystals if the orthorhombic or rhombohedral phase is shifted to room temperature.

It is well known that the phase transition temperatures in BaTiO_3 can be altered by doping with either A or B site substitutions.⁴ Zirconium is one element that pinches the transition temperatures so that the rhombohedral–orthorhombic and orthorhombic–tetragonal phase transition temperatures are raised while the Curie temperature is lowered.^{4–6} By varying the amount of dopant it is possible to stabilize either the rhombohedral and orthorhombic phases at room temperature.^{5,6} In this work Zr-doped BaTiO_3 crystals were produced and the properties of resultant crystals poled along the pseudocubic [001] direction were investigated.

Preparation of single crystals is difficult and time consuming for many systems, including BaTiO_3 . In this work, templated grain growth was used to produce crystals with Zr concentrations between 4.5 and 8.5 mol % for rapid assessment of crystals of varying composition. This section describes the synthesis and piezoelectric properties of Zr-doped BaTiO_3 single crystals grown by templated grain growth (TGG).

II. EXPERIMENTAL PROCEDURE

Single crystal BaTiO_3 cutoffs (Lockheed Sanders Inc., Nashua, NH) were used as template crystals for TGG. The orientation of the crystals was determined by four-circle x ray or backscattered x-ray Laue techniques. The crystals were sectioned along {001} faces using a diamond saw to sizes in the range of a few mm in size $\times 0.3$ mm thick. One side of the template was polished with 1 μm diamond paste.

In prior research, it was demonstrated that BaTiO_3 crystals could be grown using TGG at 1350 °C, above the eutectic temperature, with a Ti-rich initial powder. This resulted in the formation of a liquid phase at the growth temperature that was found to accelerate the growth process. Therefore, a titanium-rich BaTiO_3 powder with a proper amount of Zr was used for TGG. The powder was obtained by mixing BaCO_3 (0.1 μm , Sakai Chemical Co., Sakai, Japan), TiO_2 (0.5 μm , Ishihara Chemical Co., Kobe, Japan), and ZrO_2

^{a)}Electronic mail: paulr@psu.edu

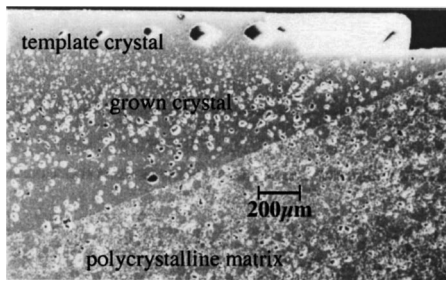


FIG. 1. Scanning electron micrograph of BaTiO₃ template crystal, Ba(Zr_{0.05}Ti_{0.95})O₃ grown crystal, and the Ti-rich polycrystalline matrix Ba(Zr_{0.05}Ti_{0.95})O₃+3 mol % TiO₂ after 30 h at 1350 °C.

(0.05 μm, TAM Ceramics Inc., Niagara Falls, NY) powders in a Nalgene bottle with an aqueous dispersant (Tamol, T963), and high density ZrO₂ media at a pH of 10 in DI-H₂O. The slurry was milled overnight and then dried in a Pyrex pan. The powder was calcined in O₂ at 1150 °C for 4 h, followed by further heating in air at 1200 °C for 2 h. The final powder was attrition milled for 16 h and then sieved to less than 45 μm (−325 mesh) prior to being mixed with an organic binder (Acryloid B-7 MEK, Rohm & Haas, Philadelphia, PA). Pellets were pressed uniaxially at 140 MPa followed by cold isostatic pressing at 276 MPa and sintering at 1300–1350 °C for 2 h in air. The grain size of the 4.5 and 5.0 mol % Zr-doped BaTiO₃ sintered ceramics was ~15 μm and the samples were approximately 98% of theoretical density. The grain size of the 8.5 mol % Zr-doped BaTiO₃ sintered ceramics was ~25 μm and the sample was approximately 92% of theoretical density. One side of sintered polycrystalline matrix was polished with 1 μm diamond paste.

For TGG, a {100} surface of the BaTiO₃ crystal was contacted, without pressure, with the sintered polycrystalline matrix and the assemblage was heated in air to 1350 °C for 8–30 h. Cross sections of the growing crystal in the polycrystalline matrix were examined by scanning electron microscopy (SEM) (ISI Model DS 130) after polishing to 1 μm diamond paste and then thermal etching at 1300 °C for 30 min.

Grown crystals were sectioned from the template and polycrystalline matrix so that dielectric measurements were performed on the grown crystals alone (i.e., none of the original BaTiO₃ crystal remained). The pseudocubic {001} faces of grown crystals were oriented via x-ray Laue techniques and polished with 1 μm diamond paste followed by gold sputtering to form electrodes. A multifrequency meter (HP 4284A LCR meter) was used in conjunction with a computer controlled temperature chamber (Delta Design Inc., Model MK 9023) to measure the dielectric constant as a function of temperature on cooling (175 to −100 °C) at frequencies between 100 Hz and 100 kHz. Samples were poled either by field cooling (10 kV/cm) from temperatures above the dielectric maximum temperature (T_{\max}) or by applying 40 kV/cm at room temperature. High field measurements (1–50 kV/cm) included simultaneous polarization (P) and strain (S) hysteresis curves obtained using a computer-controlled modified Sawyer–Tower system and a linear variable displacement transducer (LVDT) sensor driven by a

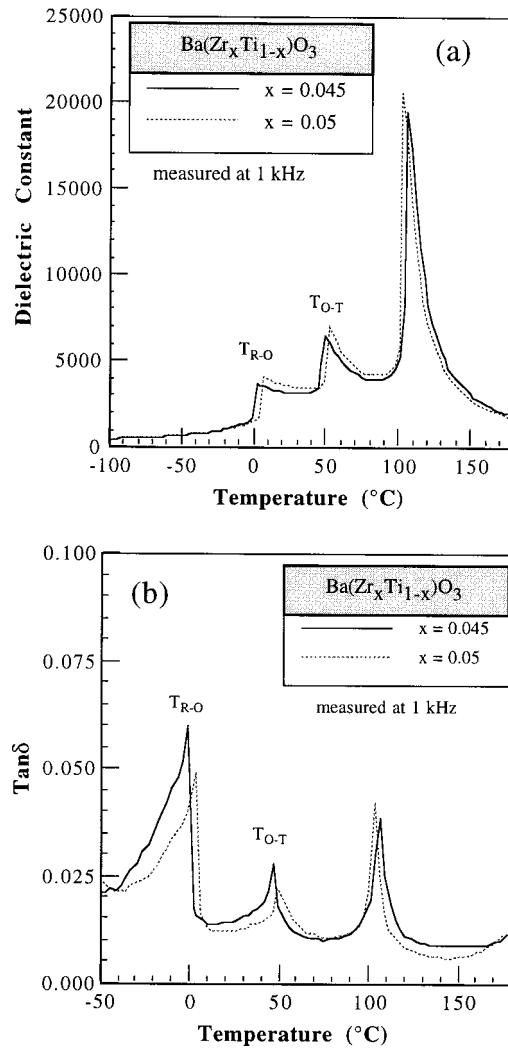


FIG. 2. Dielectric constant (a) and dielectric loss (b) as a function of temperature at 1 kHz for TGG grown Ba(Zr_xTi_{1-x})O₃ single crystals, where $x=0.045$ and 0.05 . (T_{R-O} =rhombohedral to orthorhombic transition T_{O-T} =orthorhombic to tetragonal transition).

lockin amplifier (Stanford Research Systems, Model SR830). The voltage was supplied using either a Trek 609C-6 high voltage dc amplifier or a Kepco BOP 1000M amplifier. The same system was used to measure unipolar strain curves on poled crystals oriented along the pseudocubic {001}. The value for d_{33} was estimated from the slope of the unipolar strain versus electric field (E) curve. Electromechanical coupling was measured using the IEEE Resonance Technique (ANSI/IEEE Std. 176-1978) on samples poled by field cooling above the Curie temperature and 10 kV/cm.

III. RESULTS AND DISCUSSION

Figure 1 shows a scanning electron micrograph of a cross-sectional view of the Ba(Zr_{0.05}Ti_{0.95})O₃ crystal (BZT-O5.0), the template crystal, and the polycrystalline matrix after 30 h at 1350 °C. The boundary migrated as much as 825 μm into the polycrystalline matrix. Note that the crystal growth front is no longer parallel to the initial template surface, but has grown to a habit plane, as was shown previously for growth into pure BaTiO₃ matrices.^{7,8} The grown

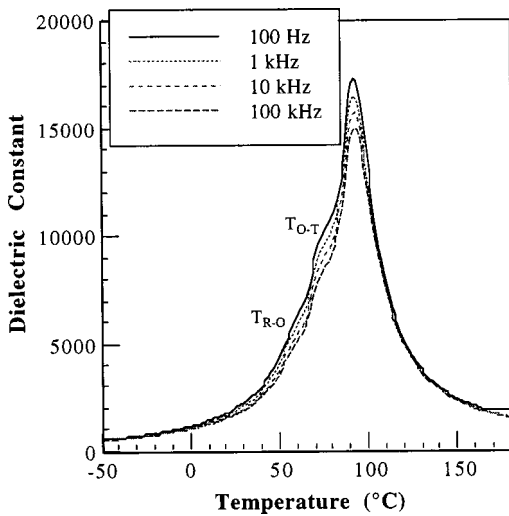


FIG. 3. Dielectric constant as a function of temperature and frequency for TGG grown $\text{Ba}(\text{Zr}_{0.085}\text{Ti}_{0.915})\text{O}_3$ single crystal.

crystal also incorporated approximately 2 vol % of the matrix porosity. The average growth rate from a $\langle 001 \rangle$ oriented template crystal after 30 h was $28 \mu\text{m/h}$. However, the initial growth rate may have been faster when the matrix grain size was $15 \mu\text{m}$. The final matrix grain size was $22 \pm 17 \mu\text{m}$, with a significant number ($\sim 10\text{--}15 \text{ vol } \%$) with a grain size $> 40 \mu\text{m}$. Coarsening of matrix grains is known to decrease the driving force associated with boundary migration during TGG. As indicated by the variable porosity entrapped in the crystal, the rate of growth continuously decreased with time. In the top layer of the grown crystal the pores remain abundant and $\sim 5\text{--}10 \mu\text{m}$ in size. After the growth rate slowed, fewer pores are trapped and those that remain coalesced before entrapment.

Figure 2 shows the dielectric constant (a) and dielectric loss (b) as a function of temperature and mol % zirconium at 1 kHz. The samples showed very little dispersion as a function of frequency and therefore only the 1 kHz values are shown. As seen in polycrystalline Zr-doped BaTiO_3 , the transition temperatures are pinched with increasing mol % zirconium.^{4-6,9} The 4.5 (BZT-O4.5) and 5.0 (BZT-O5.0) mol % Zr sample show distinct transition temperatures with both the rhombohedral-orthorhombic and orthorhombic-tetragonal transition temperatures shifted up by approximately 80°C ($T_{R-O}=0^\circ\text{C}$) and 45°C ($T_{O-T}=50^\circ\text{C}$), respectively. The amount of shift is similar to the amount of shift (75 and 49°C , respectively) predicted by Jaffe *et al.*⁴ for these compositions. The result of this shift is that the orthorhombic phase is stabilized at room temperature. The Curie temperature for the 4.5 and 5.0 mol % Zr samples shifted down by approximately 20°C ($T_C=110^\circ\text{C}$), also similar to the shift (21°C) shown by Jaffe *et al.*⁴ The room temperature dielectric constants are approximately 3200 and 3500 for unpoled BZT-O4.5 and BZT-O5.0, respectively. The room temperature dielectric loss is approximately 0.013–0.016 for both materials. What is also important to note, as clearly observed in Fig. 2, is the effect of a small change of 0.5 mol % Zr doping on the pinching behavior. This shows that the small change in matrix composition was

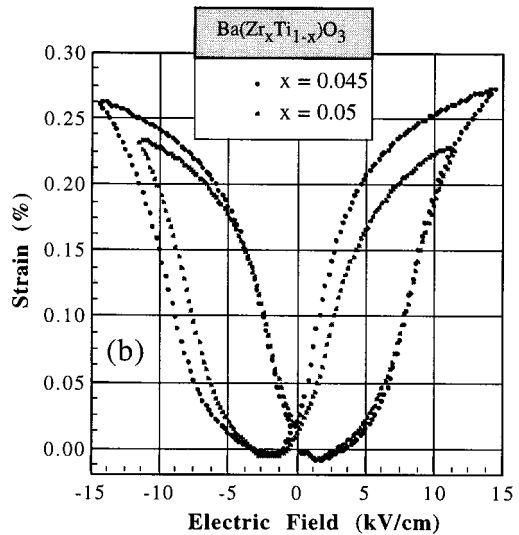
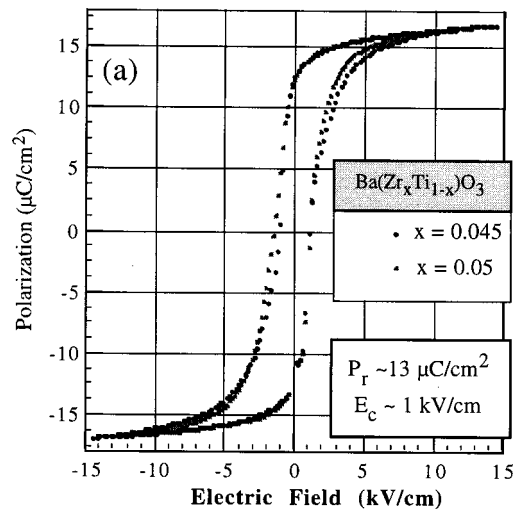


FIG. 4. Polarization (a) and strain hysteresis (b) as a function of electric field for $\langle 001 \rangle$ oriented TGG $\text{Ba}(\text{Zr}_x\text{Ti}_{1-x})\text{O}_3$ single crystals, where $x=0.045$ and 0.05 .

reflected in the grown crystal. Above the dielectric maximum temperature, T_{max} , the Curie-Weiss law is obeyed with Curie constants and Curie-Weiss temperatures of $1.4 \times 10^5^\circ\text{C}$ and 104°C for BZT-O4.5 and $1.3 \times 10^5^\circ\text{C}$ and 102°C for BZT-O5.0, respectively; i.e., $\epsilon_{R(\text{BZT-O4.5})} = 1.4 \times 10^5^\circ\text{C}/(T - 104^\circ\text{C})$ and $\epsilon_{R(\text{BZT-O5.0})} = 1.3 \times 10^5^\circ\text{C}/(T - 102^\circ\text{C})$.

Figure 3 shows the dielectric constant as a function of temperature and frequency for the crystal with 8.5 (BZT-R8.5) mol % Zr. The room temperature dielectric loss was ~ 0.05 . The dielectric response is pinched even more than for BZT-O4.5 and BZT-O5.0 and the transition behaviors are more diffuse. The rhombohedral-orthorhombic and orthorhombic-tetragonal transition temperatures shifted up by 135°C ($T_{R-O}=55^\circ\text{C}$) and 65°C ($T_{O-T}=70^\circ\text{C}$), respectively. The rhombohedral phase is stabilized at room temperature as a result of these shifts. T_{max} is shifted down by approximately 43°C ($T_{\text{max}}=90^\circ\text{C}$). These shifts in temperature are also similar to the shifts (106 , 59 , and 40°C , respectively) given by Jaffe *et al.*⁴

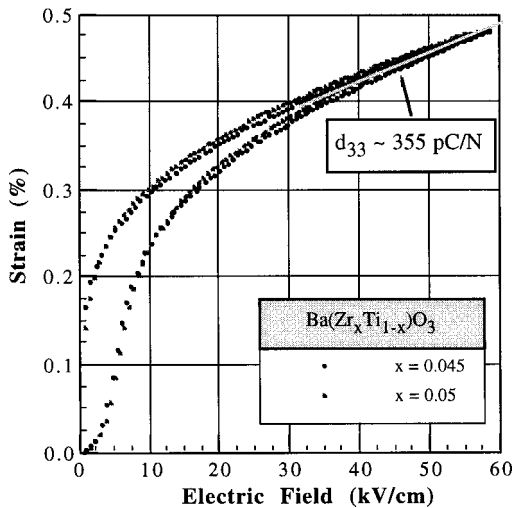


FIG. 5. Unipolar strain hysteresis as a function of electric field for (001) oriented TGG $\text{Ba}(\text{Zr}_x\text{Ti}_{1-x})\text{O}_3$ single crystals, where $x=0.045$ and 0.05 .

Figure 4 shows the polarization and strain behavior for BZT-O4.5 and BZT-O5.0 crystals oriented along the pseudocubic (001) as a function of electric field at room temperature. Orthorhombic BZT-O4.5 and BZT-O5.0 crystals have remanent polarizations (P_r) and coercive fields (E_c) of approximately $13 \mu\text{C}/\text{cm}^2$ and $1 \text{ kV}/\text{cm}$, respectively. The coercive field is lower and remanent polarizations higher^{5,9} than reported for ceramics with similar composition, which is expected for a single crystal of this orientation. In the orthorhombic phase, the polarization vector is oriented along the pseudocubic (110) direction, the magnitude of this vector is obtained by multiplying the P_r value from Fig. 4 with $\sqrt{2}$, which results in a value of $18 \mu\text{C}/\text{cm}^2$.

For the Zr-doped crystals measured here, a crystallographically engineered macrosymmetry 4 mm is expected for poling along the pseudocubic (001) axis, similar to the case of rhombohedral relaxor-PT crystals.¹ As shown in Fig. 4(a), the top of the hysteresis loop is more rounded than in the case of relaxor-PT crystals. This indicates that the crystal partially depoles near zero field. The stability of the domain state was not studied.

Figure 5 shows the unipolar strain behavior at room temperature for BZT-O4.5 and BZT-O5.0 crystals poled and excited along the pseudocubic (001) as a function of electric field. Both crystals show maximum strain levels of approximately 0.48% at a maximum field of $\sim 60 \text{ kV}/\text{cm}$, which includes $\sim 0.35\%$ strain associated with domain reorientation. After saturation, the strain behavior from 30–60 kV/cm corresponds to a d_{33} of 355 and 340 pC/N for BZT-O4.5 and BZT-O5.0, respectively.

Figure 6 shows the polarization and strain behavior for (001) oriented BZT-R8.5 as a function of electric field at room temperature. The larger hysteresis in the P vs E curve [Fig. 6(a)] relative to that for the orthorhombic crystals may be a result of inferior crystal quality, i.e., a greater volume of pores (BZT-R8.5 ~ 8 vol %, BZT-O4.5 ~ 2 vol %) and/or a higher space charge contribution to the dielectric displacement. Although $P_r \sim 10 \mu\text{C}/\text{cm}^2$ in Fig. 6(a), the top of the hysteresis loop is more rounded than for orthorhombic crys-

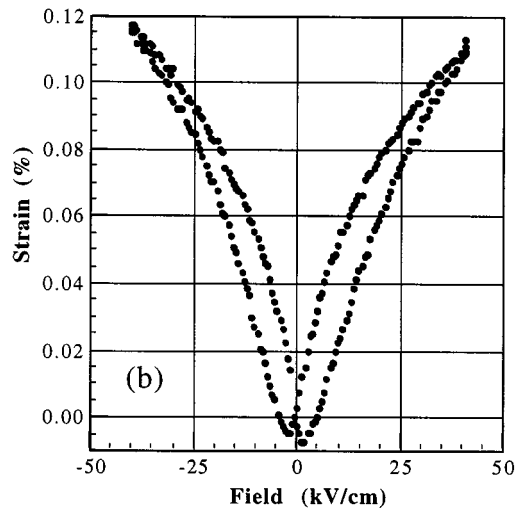
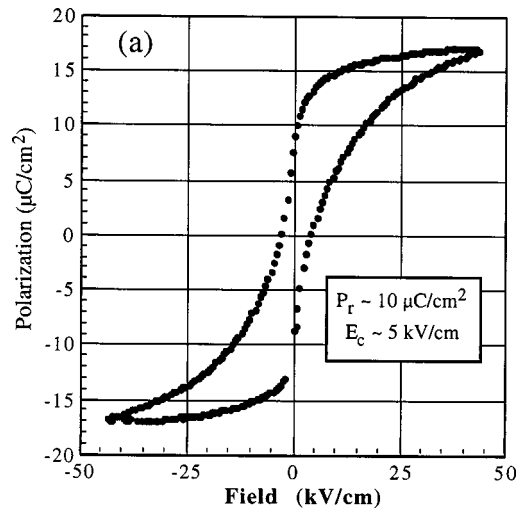


FIG. 6. Polarization (a) and strain hysteresis (b) as a function of electric field for (001) oriented TGG $\text{Ba}(\text{Zr}_{0.085}\text{Ti}_{0.915})\text{O}_3$ single crystal.

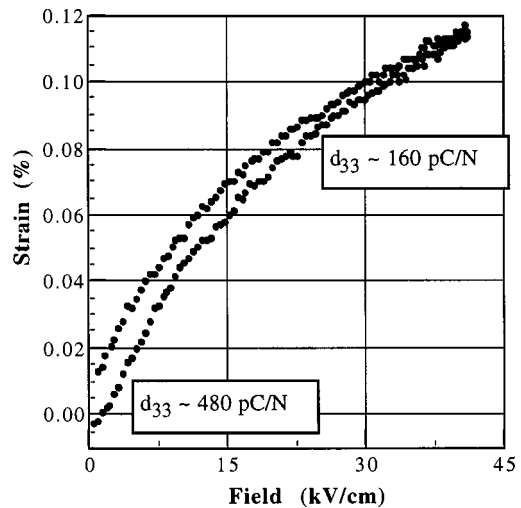


FIG. 7. Unipolar strain hysteresis as a function of electric field for (001) oriented TGG $\text{Ba}(\text{Zr}_{0.085}\text{Ti}_{0.915})\text{O}_3$ single crystal.

TABLE I. Effective electromechanical coupling data for 4.5 mol % Zr-doped orthorhombic BaTiO₃ single crystal, oriented along the pseudocubic ⟨001⟩, grown by TGG.

dc bias (kV/cm)	Freq. constant (Hz m)	k_{33}	ϵ_{33}^T	S_{33}^D (10^{-12} m ² N ⁻¹)	S_{33}^E (10^{-12} m ² N ⁻¹)	d_{33} (pC/N)
4.6	1691	0.74	770	14.5	31.7	340
1.0	1689	0.74	730	14.6	31.7	330

tals. In the rhombohedral phase, the polarization vector is oriented along the pseudocubic ⟨111⟩ direction, the magnitude of this vector is obtained by multiplying the P_r value from Fig. 6 with $\sqrt{3}$, which results in a value of 17 $\mu\text{C}/\text{cm}^2$.

The unipolar strain behavior at room temperature for a ⟨001⟩ poled rhombohedral crystal is shown in Fig. 7. d_{33} calculated from the slopes of unipolar strain versus E curves were a function of electric field, i.e., d_{33} became a maximum (~ 480 pC/N) at ~ 10 kV/cm, but decreases and subsequently saturates to 160 pC/N at $E > 30$ kV/cm. The high initial value is due, at least in part, to domain reorientation. Beyond that point, as an electric field along ⟨001⟩ prefers the tetragonal polar phase, it is possible that a modest bias field results in the transition from rhombohedral to tetragonal phase. It is noteworthy to mention that the high field $d_{33} \sim 160$ pC/N is similar to that of a single domain tetragonal BaTiO₃ crystal. This field-induced phase transition may be ascribed to the pinching effect, that is, the consequent decrease in free energy difference among polymorphic rhombohedral, orthorhombic, tetragonal, and cubic phases.

The electromechanical coupling data for 4.5 mol % Zr-doped orthorhombic BaTiO₃ single crystal (BZT-O4.5) grown by TGG is shown in Table I. After poling, no resonance was observed for electromechanical coupling measurements. Under application of a 950 V dc bias during the measurement, the values as shown in Table I were obtained, showing k_{33} and d_{33} values of 0.74 and 340 pC/N, respectively. During removal of the field the values remained essentially constant down to 200 V (1.0 kV/cm), also shown in Table I. However, upon removal of all electric field, once again no resonance was detected after a few seconds. Therefore it was necessary to apply a dc bias to stabilize a domain state. The value for d_{33} is in close agreement with the value for d_{33} determined by unipolar strain data. The values for the dielectric constant and elastic compliances, S_{ij}^D (open circuited sample) and S_{ij}^E (close circuited sample), are higher than found for pure BaTiO₃ single crystals.

IV. CONCLUSIONS

In this work, single crystals of Zr-doped BaTiO₃ were prepared using TGG for 30 h at 1350 °C. It is encouraging that TGG can be applied even in doped systems, so that the composition of the grown crystal has the same composition as the ceramic matrix. Room temperature orthorhombic (BZT-O4.5, BZT-O5.0), and rhombohedral (BZT-R8.5) crystals were successfully stabilized using 4.5–5.0 and 8.5 mol % Zr, respectively. Orthorhombic crystals exhibited a room temperature dielectric constant and dielectric loss of approximately 3500 and 0.01, as well as remanent polarizations and coercive fields of 13 $\mu\text{C}/\text{cm}^2$ and 1 kV/cm, respec-

tively. High field d_{33} values up to 355 pC/N were observed. This value was supported by resonance measurements, where a d_{33} value of 340 pC/N was observed. A k_{33} value of 0.74 was obtained under dc bias. The d_{33} and k_{33} values calculated for BZT-O4.5 (340–355 pC/N and 0.74, respectively) are almost twice the value of most nonlead materials with similar T_{max} and approaching polycrystalline PZT-5A's (DOD-type II).¹ Although the maximum d_{33} , as high as 480 pC/N (calculated from the S vs E curves) for BZT-R8.5 is observed at low electric field due to domain reorientation, under additional increase in bias, the rhombohedral phase is probably converted to tetragonal due to the small energy difference between the two associated with the pinching effect. When the orthorhombic or rhombohedral phase is stabilized to room temperature to utilize crystallographic engineering for piezoelectric performance enhancement, the phase relationships and T_{max} must be properly engineered to ensure phase stability, i.e., due to the field-induced phase transition in the rhombohedral crystals the high field measurements (field induced tetragonal phase) may not correlate well with low field measurements (rhombohedral phase). Both BZT-O BZT-R samples show high piezoelectric coefficients and an improvement in piezoelectric properties over what is currently available for nonlead systems, as a result of crystallographic engineering.

It is possible that the properties of these crystals may be improved further. In particular, better understanding of the role of crystal orientation and phase relationships on the stability of the domain state is necessary and could lead to improved composition selection. In addition, it is possible that eliminating the porosity from the crystals would result in improved electromechanical properties.

ACKNOWLEDGMENTS

Financial support from the Defense Advanced Research Projects Agency on AFSOR Grant No. F49620-94-1-0428 and on ONR Grant No. N00014-98-1-0527 are gratefully acknowledged.

¹S.-E. Park and T. R. Shrout, J. Appl. Phys. **82**, 1804 (1997).

²S. Wada, S.-E. Park, L. E. Cross, and T. R. Shrout, J. Korean Phys. Soc. **32**, S1290 (1998).

³S.-E. Park, S. Wada, L. E. Cross, and T. R. Shrout, Appl. Phys. Lett. (to be published).

⁴B. Jaffe, W. R. Cook, and H. L. Jaffe, in *Piezoelectric Ceramics* (Academic, New York, 1971), Vol. 3, pp. 49–114.

⁵D. Hennings and A. Schnell, J. Am. Ceram. Soc. **65**, 539 (1982).

⁶R. C. Kell and N. J. Hellicar, *Acustica* **6**, 235 (1956).

⁷P. W. Rehrig, G. L. Messing, and S. Trolier-McKinstry (unpublished).

⁸T. Yamamoto and T. Sakuma, J. Am. Ceram. Soc. **77**, 1107 (1994).

⁹T. R. Armstrong, L. E. Morgens, A. K. Maurice, and R. C. Buchanan, J. Am. Ceram. Soc. **72**, 605 (1989).